Experiments with neutron induced neutron emission from U-235, Pu-239, and graphite

Yaron Danon[1,*], *Ezekiel* Blain[1], *Kumar* Mohindroo[1], *Matt* Devlin[2], *Keegan* J.Kelly[2], *Jaime* Gomez[2], and *John* O'Donnell[2]

[1]Gaerttner LINAC Center, Rensselaer Polytechnic Institute, Troy, NY 12180, USA
[2]P-27, Los Alamos National Laboratory, NM 87545, USA

Abstract. A neutron induced neutron emission experiment was conducted as the Los Alamos Neutron Science Center (LANSCE) facility at Los Alamos National Laboratory (LANL). In this experiment, a sample was placed in a well collimated neutron beam and was surrounded by an array of 28 fast neutron detectors (EJ-309). The experiment was performed with a neutron flight path of 21.5 m from the source to the sample, and 1 m from the sample to the detectors. The neutron emission from the sample was measured as a function of neutron time of flight covering an incident energy range from 0.7- 20 MeV. The samples included U-235, Pu-239, carbon (graphite), and blanks that matched the encapsulation of the sample. The measured samples were constantly cycled in and out of the neutron beam. This type of experiment measures neutron emission from all reactions occurring in the sample such as fission and elastic and inelastic scattering. Similar to the methodology previously developed at RPI [1], the measurements were compared with detailed simulations of the experiment using different cross section evaluations for the sample. The observed differences can be attributed to the evaluated neutron cross section and angular distributions. The carbon sample was used as a reference to validate both the experiment and simulation methodology and showed good agreement between experiments and simulations. A review of the experimental setup, analysis methods, and some of the results will be presented.

1 Introduction

The uncertainty in evaluations of neutron induced reactions propagates to quantities calculated using these data such as the multiplication factor for a critical system, or leakage rates for critical or other nuclear systems. The uncertainty in computed quantities is a function of the uncertainty in neutron reactions and neutron angular distributions. In order to test the performance of nuclear data evaluation, different benchmark experiments are usually used; they include measurements of the multiplication factor, integral neutron flux (activation), neutron leakage, and transmission. In this work, we discuss a neutron induced neutron emission quasi-differential measurements that can be used to test the nuclear data of neutron scattering angular distributions and cross sections.

A quasi-differential experiment with high sensitivity to neutron scattering was previously developed at Rensselaer Polytechnic Institute (RPI) [1]. In this experiment, an array of 8 liquid scintillation detectors (EJ-301) was positioned at different angles around a sample of the material being measured. A neutron beam from the RPI LINAC hit the sample and scattered neutrons are detected using the time of flight (TOF) method. The distance between the neutron source and sample and the sample to the detector were 30 m and 0.5 m, respectively. Usually two detectors measured the same angle and the incident neutron energy covered the range from 0.5-20 MeV. The results of such experiments were compared to MCNP® 6.1 [2] simulations of the experiments using different evaluations for the sample material, and the differences between simulations and experiment indicate energies and angles where improvement is needed. An assessment of the systematic uncertainty in this methodology was derived from a sample of carbon that was measured with the sample of interest in all experiments. Previous measurements were reported for Mo [1], Zr [3], U-238 [4], Fe [5], Mo and Be [6] and Pb [7]. For the case of Fe it was also possible to obtain the ratio of inelastic to elastic scattering for the first inelastic state, and the elastic only scattering yield [5]. Scattering data from these measurements was used in evaluation of U-238 for the CIELO project [8] and validation of the ENDF/B-8.0 evaluations of Be [9].

Here we describe an experiment that explores the use of a similar methodology to measure neutron induced neutron emissions form sample of U-235 and Pu-239. Using samples with large fission cross sections means that the measured neutrons include neutrons from fission and other reactions such as neutrons from elastic (n,n) and inelastic (n,n') collisions, and (n,xn) reactions. Fission cross sections are easier to measure and thus know much better than + other neuron emitting reactions; therefore, the

*e-mail: danony@rpi.edu

information from this measurements can be used to infer issues with other neutron emitting reactions and their angular distributions.

2 Experimental setup

The experiment described here is a second iteration of the experiment described in [10]. The experiment was performed using the Chi-Nu liquid scintillation detector array [11] at Los Alamos National Laboratory (LANL), the detector array was conFigured with 28 EJ-309 liquid scintillation detectors (with liquid cell dimensions; 7.8 cm dia.and 5.08 cm thick) positioned at 9 different angles covering the range from 30 deg, to 150 deg. configured with 2 to 4 detectors measuring at the same angle. An illustration of the geometry is shown in Figure 1.

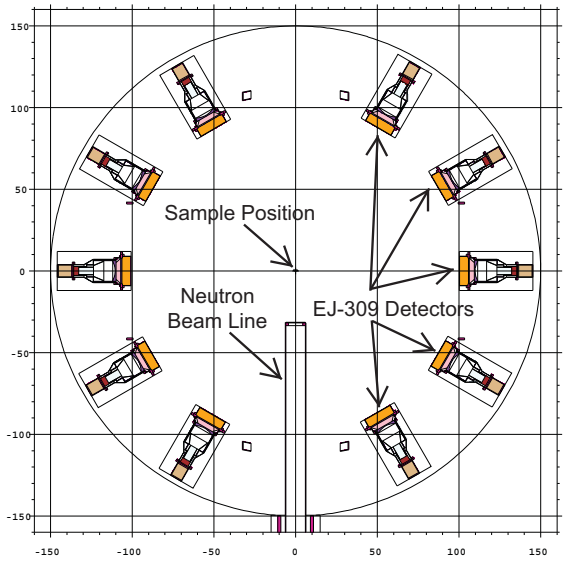

Figure 1. Horizontal cut of the geometry of the experiment (plotted using MCNP® 6.1) showing the sample position and the surrounding detector array.

The signals from the detectors were connected to CAEN VX1730B 14 bit digitizers operating at a sampling rate of 500 MHz (2 ns/channel). The flight path from the neutron source to the sample and the sample to detector were 21.5 m and 1 m, respectively. A neutron beam was provided at an average rate of 100 Hz with a macro pulse length of 625 Hz that included 347 micro pulses separated by 1.8 μs. Due to the 1.8 μs pulse spacing, the lowest possible incident neutron energy which could be measured was about 0.7 MeV. A U-235 fission chamber [12] was placed at a flight path distance of 28.75 m and was used to measure the beam energy spectrum that is needed for the simulation of the experiment.
An automated sample changer was used to place the U-235, Pu-239 and carbon (graphite) samples. Additionally, an open position or a blank (sample enclosure) was also measured. During the experiment each sample was measured for 10 minutes cycling between the sample of interest (U-235 or Pu-239), the Carbon reference sample, the sample encapsulation blank, and open (nothing in beam). Such rotation of the samples averages long term variation is the neutron beam flux intensity and allow to use the carbon sample to normalize the simulations to the experiment.

2.1 Samples

Characteristics of the of U-235, Pu-239, and carbon sample used are given in Table 1. The U-235 sample was in a form of a truncated cone and was covered by a total of 2 mil (0.00508 cm) aluminum foil, a blank with the same thickness of aluminum was also measured. The Pu-239 sample was cylindrical with 2.55 cm diam. and 0.307 cm thick encapsulated in a stainless steel container [13], a blank with the same container and 0.47 g of Pu-239 was also measured. The carbon sample was cylindrical; 3.8 cm diam. and 3.5 cm long.

Table 1. Mass and enrichment of the samples. The mass measurements were assumed to have 1% uncertainty. The Pu-239 sample was an alloy with 3.6 at.% of Ga [13]

Sample	Mass [g]	Enrichment [wt%]
U-235	49.5 ± 0.5	93% U-235
Pu-239	24 ± 0.2	93.9% Pu-239, 5.9% Pu-240
Pu-239 blank	0.47 ± 0.2	93.9% Pu-239, 5.9% Pu-240
Carbon	38.6 ± 0.4	

2.2 Data analysis

The data were collected and pulse shaped discrimination was utilized in order to differentiate the neutron signal from the gamma signal. The timing of the neutron event was then determined and a neutron TOF spectrum was generated for each detector and each sample. The neutron TOF spectrum of the blanks was subtracted from the sample in order to obtain the net sample counts for each detector.
To compare with the simulation, both the energy dependent flux shape, and the shape of the detection efficiency curve are required. The neutron flux shape was inferred from the reaction rate measured with the U-235 fission chamber, the flux shape is shown in Figure 2. This flux shape was used in the MCNP® 6.1 simulation of the experiment.

The neutron detection efficiency was calculated using the SCINFUL [14] code with a modification to match the density and composition of EJ-309. For validation, a measurement of the efficiency was performed using two methods; a Cf-252 fission chamber, and by scattering neutrons from a thin carbon sample, the comparison is shown in Figure 3. Due to detector time response limitation of the Cf-252 fission chamber, data was measured only up to about 5 MeV. The efficiency derived from a measurement of neutron scattering from a thin (1 mm) carbon was determined using an MCNP® 6.1 simulation of the neutron scattering to the face of the detector and used the flux

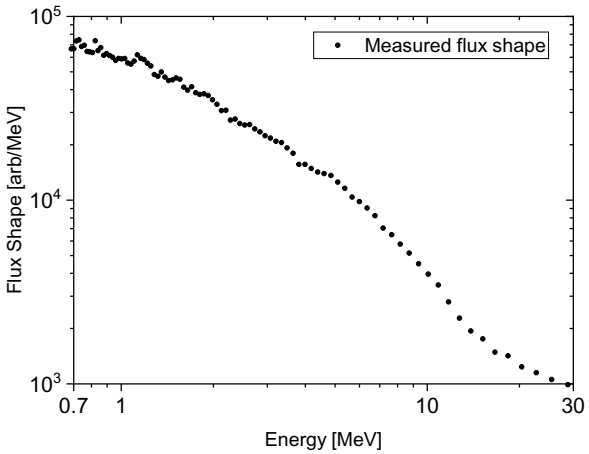

Figure 2. The neutron flux shape on the face of the sample.

shape previously determined as input. As shown in figure 3, the agreement between the experiments and simulation is very good with an exception near 1 MeV where the experiment is higher.

For the analysis presented here, the efficiency of all detectors was assumed to be the same; however, this is not necessarily the case and further analysis of the thin carbon scattering measurements may yield individual detector efficiencies.

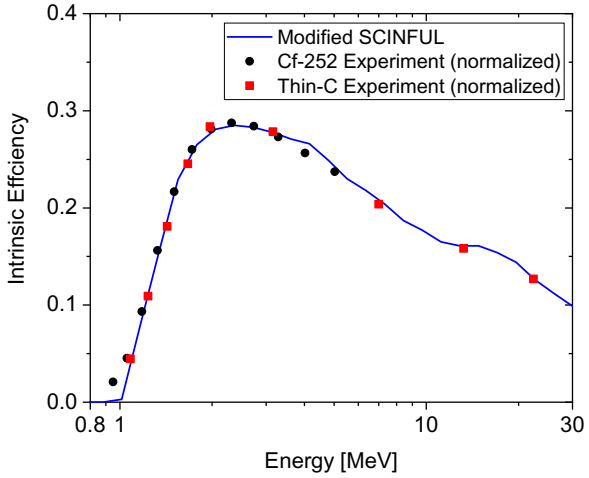

Figure 3. The energy dependent neutron detection efficiency calculated by SCINFUL and experimental results.

3 Results

The carbon reference sample was used to normalize the simulations to the experimental data. A ratio of the integrals of experiment to simulation was calculated for each detector (each angle) separately and the average was used as the normalization factor applied to the simulation. This procedure resulted in a 3% standard deviation that was used as the systematic uncertainty of this method. Larger discrepancies from the average were observed for the forward angles and the 30 deg angle was discarded. The reason for this discrepancy is possibly forward high-energy scattered neutrons from the collimation system that were not modeled accurately. The spread of the normalization factors for the carbon sample measured during the U-235 experiment are shown in Figure 4.

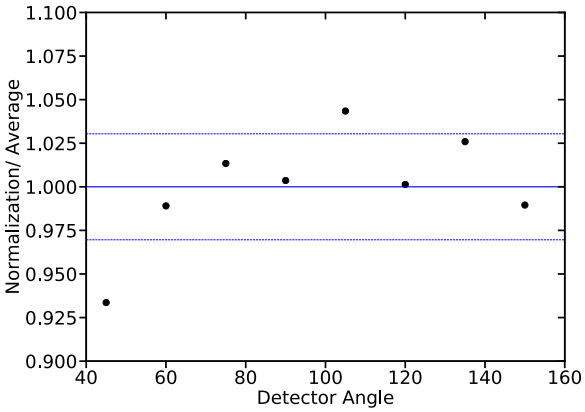

Figure 4. Normalization of carbon simulation to the experimental data measured during the U-235 experiment. The normalization TOF range was from 400 to 1400 ns. To show the spread better; the experiment to simulation ratios were normalized to the average (solid line), the dashed lines represents one standard deviation from the average.

The experimental data was compared with time dependent MCNP® 6.1 simulations and are presented for a forward and back angle in Figures 5 and 6 for U-235, and 7 and 8 for Pu-239. In these plots the bottom x-axis is the neutron TOF and the top x-axis is the approximate incident neutron energy calculated by using an effective TOF distance $L = L_1 + L2 = 21.5 + 1 = 22.5$ m. The counts on the y-axis is experimental data averaged to one 10 minute run. Two angles are shown 60 deg (forward angle) and 150 deg (back angle), the carbon experiment and simulation are in good agreement. The U-235 experiment and simulation agree reasonably well with some differences above 5 MeV. Comparing ENDF/B-VII.1 to ENDF/B-VIII.0 indicate that small differences between the evaluated libraries are observable in the simulation, overall the experiment agree better with the simulation using U-235 from ENDF/B-VIII.0.

For the Pu-239 measurement, the carbon data associated with the Pu-239 measurement is in good agreement with the simulation but the Pu-239 sample is not agreeing as good as the U-235. One issue with the Pu-239 is the sample encapsulation. In the experiment the encapsulation was addressed by measuring a similar sample with a small amount of Pu-239 that can be subtracted from the large Pu-239 sample and thus provide some compensation for scattering from the encapsulation itself. Exact knowledge of the encapsulation geometry and material is needed as input to the simulation and was not available to the desired accuracy. Thus it is possible that some of the observed differences between the experiment and simulation could be due to modeling of the sample encapsulation. Similar to the U-235 sample, differences between the two evaluations (ENDF/B-VIII.0 and JEFF 3.3) are visible which indicates

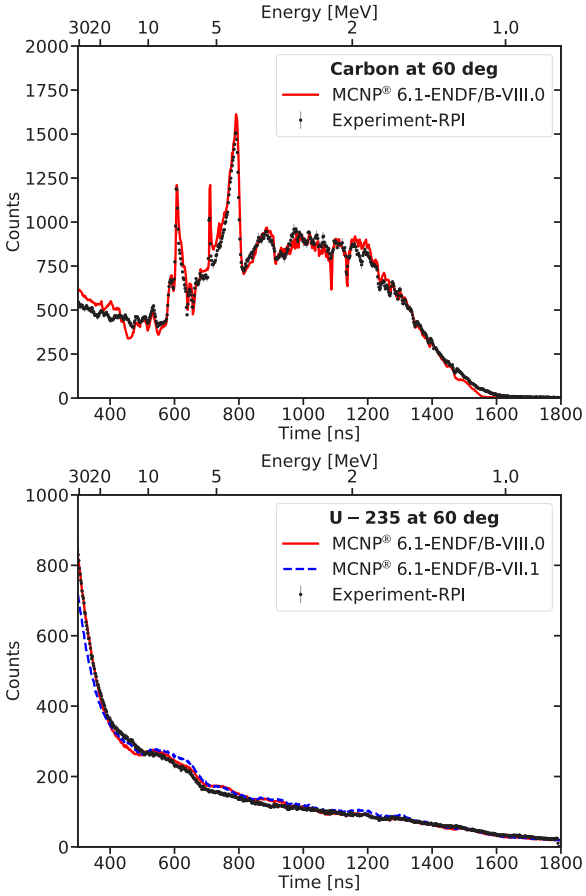

Figure 5. Results for neutron emission at 60 deg relative to the incident beam. Top shows the experimental data and simulation for carbon, bottom, experiment and simulation for the U-235 sample.

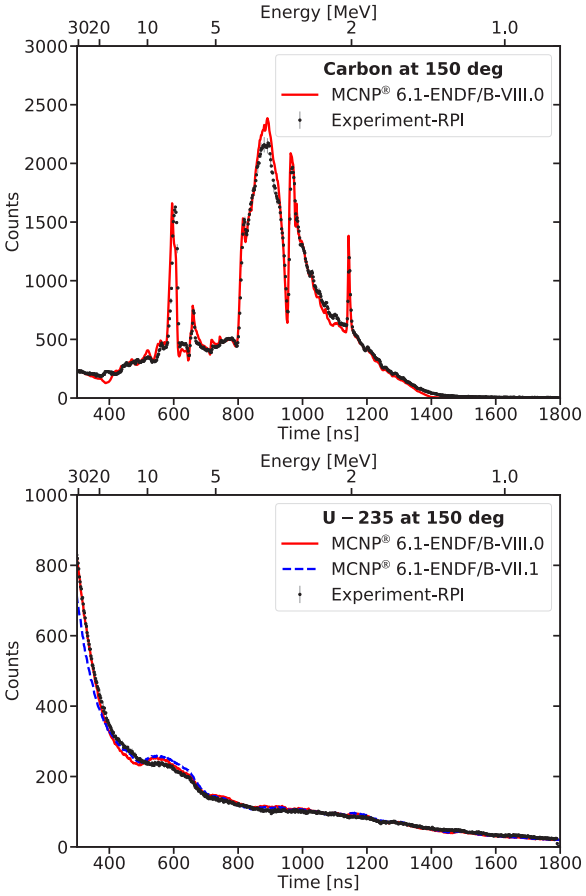

Figure 6. Results neutron emission at 150 deg relative to the incident beam. Top shows the experimental data and simulation for carbon, bottom, experiment and simulation for the U-235 sample.

that with sufficient experimental accuracy this method can help validate and improve evaluations.

4 Conclusions

Experiments to measure neutron induced neutron emission were performed at LANL using samples of U-235, Pu-239 and Carbon (graphite). The measurements were performed using the Chi-Nu liquid scintillation detector array configured with 28 EJ-309 detectors, pulse shape analysis was used to remove contributions from gammas. Data were measured as a function of TOF covering to incident neutron energy from 0.7 to 30 MeV. Simulation of the experiment using MCNP® 6.1 were normalized to the carbon data measured with the sample (U-235 or Pu-239). Comparison of the experiments and simulations shows good agreement for U-235 up to about 10 MeV, above this energy simulations using ENDF/B-VIII.0 agrees better than ENDF/B-VII.1. For Pu-239 the agreement is not as good as the U-235, however the experimental data might be sufficient to differentiate small differences observed between ENDF/B-VIII.0 and JEFF-3.3.

A more comprehensive analysis of the data including the effect of room return is still in progress at the time of writing this summary. This was the first experiment of this type for U-235 and Pu-239; repeating the experiment with better samples and with more information on the encapsulation and surrounding will be beneficial for reducing uncertainties.

Acknowledgment

This work by the DOE-SSAA award no. DE-NA0002906, and by the US Department of Energy through the Los Alamos National Laboratory. Los Alamos National Laboratory is operated by Triad National Security, LLC, for the National Nuclear Security Administration of U.S. Department of Energy (Contract No. 89233218CNA000001). Any opinions, findings, and conclusions or recommendations expressed in this publication are those of the author(s) and do not necessarily reflect the views of DOE.

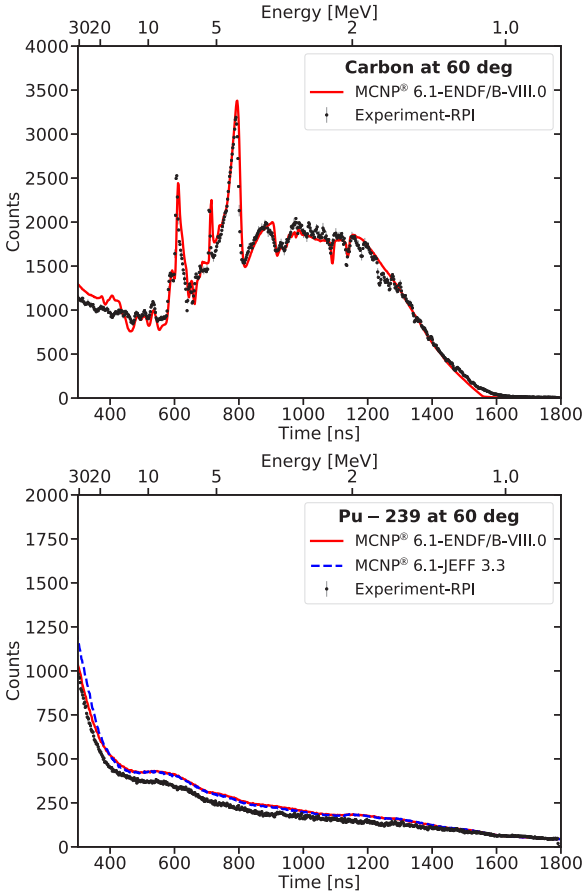

Figure 7. Results for neutron emission at 60 deg relative to the incident beam. Top shows the experimental data and simulation for carbon, bottom, experiment and simulation for the Pu-239 sample.

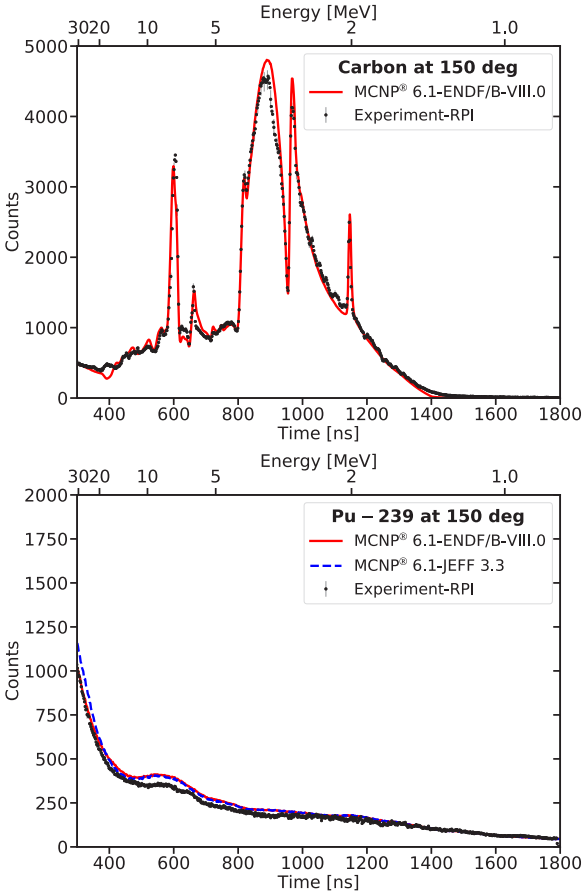

Figure 8. Results for neutron emission at 150 deg relative to the incident beam. Top shows the experimental data and simulation for carbon, bottom, experiment and simulation for the Pu-239 sample.

References

[1] F. Saglime, Y. Danon, R. Block, M. Rapp, R. Bahran, G. Leinweber, D. Barry, N. Drindak, Nucl. Instrum. Methods Phys. Res., Sect. A **620**, 401 (2010)

[2] J.T. Goorley, M.R. James, T.E. Booth, F.B. Brown, J.S. Bull, L.J. Cox, J.W.J. Durkee, J.S. Elson, M.L. Fensin, R.A.I. Forster et al., LA-UR-13-22934 (2013)

[3] D.P. Barry, G. Leinweber, R.C. Block, T.J. Donovan, Y. Danon, F.J. Saglime, A.M. Daskalakis, M.J. Rapp, R.M. Bahran, Nucl. Sci. Eng. **172**, 188 (2013)

[4] A. Daskalakis, R. Bahran, E. Blain, B. McDermott, S. Piela, Y. Danon, D. Barry, G. Leinweber, R. Block, M. Rapp et al., Ann. Nucl. Energy **73**, 455 (2014)

[5] A. Daskalakis, E. Blain, B. McDermott, R. Bahran, Y. Danon, D. Barry, R. Block, M. Rapp, B. Epping, G. Leinweber, Annals of Nuclear Energy **110**, 603 (2017)

[6] A. Daskalakis, E. Blain, G. Leinweber, M. Rapp, D. Barry, R. Block, Y. Danon, EPJ Web Conf. **146**, 11037 (2017)

[7] A.E. Youmans, J. Brown, A. Daskalakis, N. Thompson, A. Welz, Y. Danon, B. McDermott, G. Leinweber, M. Rapp, AccApp 15, Washington, DC pp. 355–360 (2015)

[8] R. Capote, A. Trkov, M. Sin, M. Pigni, V. Pronyaev, J. Balibrea, D. Bernard, D. Cano-Ott, Y. Danon, A. Daskalakis et al., Nuclear Data Sheets **148**, 254 (2018), special Issue on Nuclear Reaction Data

[9] D. Brown, M. Chadwick, R. Capote, A. Kahler, A. Trkov, M. Herman, A. Sonzogni, Y. Danon, A. Carlson, M. Dunn et al., Nuclear Data Sheets **148**, 1 (2018), special Issue on Nuclear Reaction Data

[10] K. Mohindroo, E. Blain, Y. Danon, S. Mosby, M. Devlin, Transactions of the American Nuclear Society **115**, 701 (2016)

[11] K.J. Kelly, T. Kawano, J.M. O'Donnell, J.A. Gomez, M. Devlin, D. Neudecker, P. Talou, A.E. Lovell, M.C. White, R.C. Haight et al., Phys. Rev. Lett. **122**, 072503 (2019)

[12] S. Wender, S. Balestrini, A. Brown, R. Haight, C. Laymon, T. Lee, P. Lisowski, W. McCorkle, R. Nelson, W. Parker et al., Nuclear Instruments and Methods in Physics Research Section A: Accelerators, Spectrometers, Detectors and Associated Equipment **336**, 226 (1993)

[13] J.E. Lynn, G.H. Kwei, W.J. Trela, V.W. Yuan, B. Cort, R.J. Martinez, F.A. Vigil, Phys. Rev. B **58**, 11408 (1998)
[14] J.K. Dickens, ORNL-6463 (1988)